2nd International Conference Frontiers in Diagnostic Technologies At Laboratori Nazionali di Frascati, ITALY [28th November to 30th November, 2011]

A PASSIVE CHARGE EXCHANGE DIGNOSTICS AT ADITYA TOKAMAK FOR ION TEMPERATURE ESTIMATION USING ELECTROSTATIC PARALLEL PLATE ANALYSER [EPPA]

Authors

Kumar Ajay*, Santosh P. Pandya, Priyanka Mishra, Rajani D. Dhingra and J. Govindarajan

*Author's Email: kumarajay.ipr@gmail.com

Institute For Plasma Research
Bhat, Gandhinagar-382428
GUJARAT (INDIA).

Introduction

Ion temperature in hot plasmas may be measured by several well developed methods [1], each having its advantages and disadvantages. Ion temperature measurement methods based on monitoring of Charge Exchange (CX) Neutrals are well established techniques [2, 3, 5, 7-18, 20 & 21]. A convenient method is to obtain CX-Neutral Mass/Energy resolved spectra using Electro-Magnetic filed [17]. Energetic neutral particles that are formed due to charge exchange of plasma ions with neutral atoms, escape the plasma readily since neutral do not interact with electric or magnetic fields of the confinements in tokamaks.

$$H^{+}_{hot} + H^{0}_{cold} \rightarrow H^{0}_{hot} + H^{+}_{cold}$$

Samplings of such neutral atoms which are re-ionized and analyzed give the information about the plasma ion energy distribution. Even though this method has some limitations, the ion temperature estimate obtained is fairly accurate.

Description of the CX-NPA system

The analyzer box is a vacuum chamber made of 25 mm thick soft iron plates. Plate thickness is derived using the calculation given in the reference [5] to minimize the magnetic field effect during the plasma discharge.

$$B_{in} = B_{out}\frac{3r}{5\mu t} \qquad [1]$$

The vessel reduces the stray magnetic field i.e. Bin down to ~0.03 gauss in present case.

The parallel plate analyzer is placed at 45 degree close to stripping cell for a better energy resolution [4].

Channel Electron Multipliers (Amptektron made, model MD-501) are used to detect the particles [6]. The whole system is pumped down to a pressure of $2{\times}10^{-6}$ Torr by a 1000l/s turbo molecular pump (Oerlikon Leybold make, Model TURBOVAC 1100 C). The main gas load comes from the stripping cell. The viewing geometry of the analyzer has been chosen such that it samples ±0.5 cm vertically and ±1.0 cm toroidally at the plasma center. The solid angle subtended by the plasma at the stripping cell is $\sim10^{-6}$ steradians.

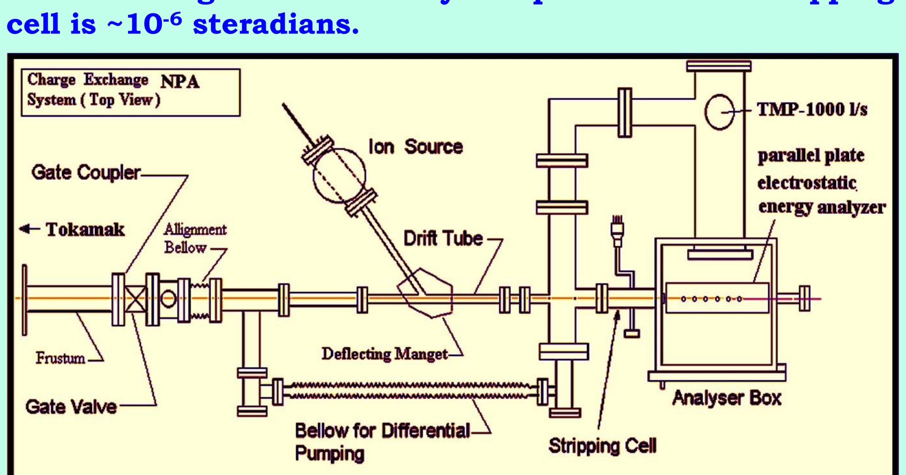

Figure-1: Schematic layout of the Aditya Charge Exchange NPA.

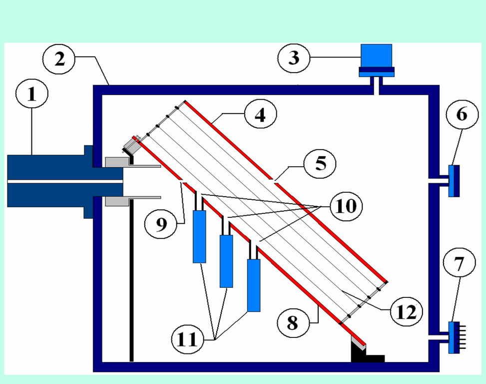

Figure-2(a): Schematic layout of Parallel plates in Analyzer box

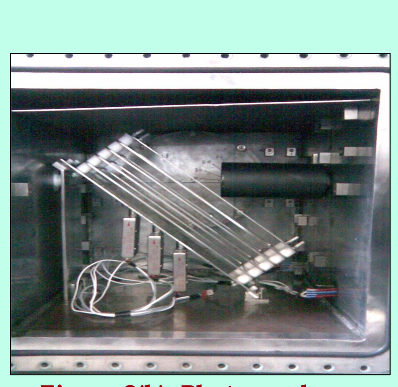

Figure-2(b): Photograph of the plates

Schematic layout of the CX-NPA and its Photograph. Components inside CX-NPA are: (1) Stripping Cell, (2) Analyzer Box, (3) Pressure Gauge, (4) Positive Plate (PP), (5) Exit aperture at PP (straight channel), (6) Alignment Window, (7) Electrical Feed through, (8) Grounded Plate (PG), (9)Entrance aperture, (10) Exit apertures at GP (Energy Channels), (11) CEM-detector, (12) Guard Rings.

Energy Calibration of CX-NPA

The relation between analyzer plate voltage V_p and corresponding focusing different energies on three energy channels is shown in Figure-6. Good agreement has been found between calculated values using equation-2 and experimental data points.. However, due to deviation in the parallelism of two parallel plates (±4 mm), slight deviation at low energy channel is observed.

Channel No.	Distance of Detector aperture from Striping Cell (Exit slit) center X_i (mm)	Energy Resolution ΔE/E Corresponding to 500 eV Beam Energy	
		Calculated $\frac{\Delta E_i}{E} = \frac{(\Delta X_0 + \Delta X_i)}{X_i}$	Experimental $\frac{\Delta E_i}{E} = \frac{FWHM \text{ of Peak}}{E}$
1	70	0.20	0.41
2	105	0.13	0.22
3	140	0.10	0.12

Table of the three energy channels and corresponding energy resolutions.

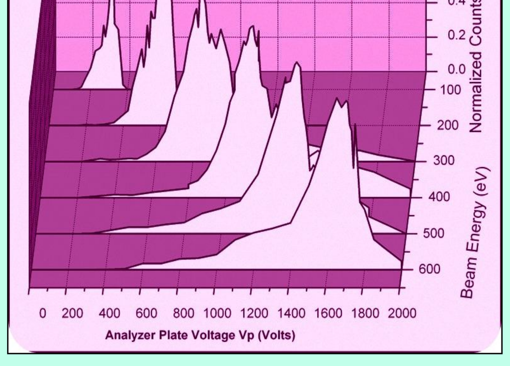

Figure-3(a): Different count peaks corresponds to different analyzer plate voltage V_p and H^+ beam energy for Cannel2. Channel Electron Multipliers (Amptektron made, model MD-501) are used to detect the particles [6].

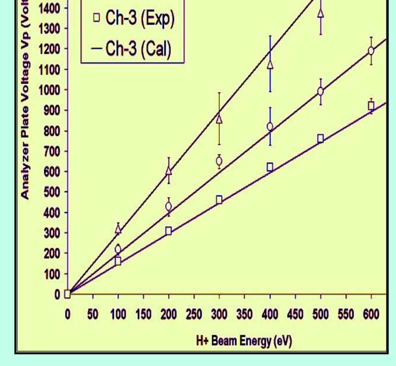

Figure-3(b): CX-NPA calibration curve Analyzer Plate Voltage (V_p) vs. Detected Energy (E) for three different channels. [Refer Eq^n 3].

Principle of Ion temperature estimation

The charged particles under the influence of a retarding field follow a parabolic path and go back to the plate PG and hit at a distance X_i from the entrance point. This range X is given by [4]

$$E = \frac{V_p}{2d}X_i \qquad [2]$$

Where d is the distance between the plates PG and PP i.e. 100 mm in present case, E is the energy of the incident particle in eV, V_p is the voltage applied to the analyser plates. Thus the particle going out through exit holes at a distance X_i would have an energy given by

$$X_i = \frac{2Ed}{V_p} \qquad [3]$$

Since the θ is too small (θ < 1°) for the ions entering into the analyzer even after experience scattering in stripping cell [8], the energy resolution is given by [4, 19 & 22]

$$\frac{\Delta E}{E} = \frac{(\Delta X_0 + \Delta X_i)}{X_i} \qquad [4]$$

Where ΔX_0 is the width of the entrance aperture (6.5 mm) and ΔX_i is the width of the exit aperture or the detector aperture (6.5 mm). It should be noted that as the range reduces energy resolution deteriorated. The analyzer is fixed at 45° with respect to the incident beam as this provides optimum energy resolution and focusing [4, 5].

The number of counts recorded at the exit of the analyser corresponding to the energy E ions

$$C(E) = \frac{\Omega}{4\pi}\eta_s\eta_t\eta_c N(E)\Delta E\Delta t \qquad [5]$$

Where Δt is the interval over which counts are collected, Ω is the solid angle subtended by the stripping cell at the plasma center, η_s is the stripping cell efficiency, η_t is the net transmission efficiency, η_c is the detection efficiency of the CEMs, ΔE is the energy resolution of the Analyser and N (E) ΔE is the number of neutrals in the energy range E +ΔE emitted per second from the volume ΔV sampled by the analyzer given by

$$N(E) = \Delta V \eta_0 \eta_+ f \sigma_{cx} v \qquad [6]$$

Where η_0 and η_+ are the neutral and ion densities respectively, σ_{cx} is the cross-section for charge exchange reaction at ion energy E, v is the relative velocity between neutrals and ion undergoing charge exchange and f is the Maxwellian distribution function given by

$$f = \frac{2}{T}\sqrt{\frac{E}{\pi T}}\exp^{-E/T} \qquad [7]$$

T being the ion temperature.

Substituting Equation-6 and 7 in Equation-5 we get the expression for the counts C (E) at a channel with energy E as

$$C(E) = \frac{\Omega}{4\pi}\eta_s\eta_t\eta_c N(E)\Delta E\Delta t \qquad [8]$$

Factoring out the energy dependent terms we get,

$$\ln F = \ln K - \frac{E}{T} \qquad [9]$$

Where F is $\frac{C(E)}{\eta_s\sigma_{cx}v\sqrt{E}\Delta E}$ and K is $\frac{\Omega}{4\pi}\Delta V \eta_s\eta_t\eta_c\eta_0\eta_+ \frac{2}{T}\sqrt{\frac{1}{\pi T}}\Delta t$ [10]

So knowing the energy dependent quantities in F (η_s, $\langle\sigma_{cx} v\rangle$, ΔE and C (E) at different E) one can obtain the inverse of the slope given by the Equation-9, as an estimate of the ion temperature.

However, the plot obtained by Equation.-9, will deviate from a straight line at lower energies because the plasma temperature is not constant along the line of sight. It peaks in the center and falls off parabolically towards the walls. Further, low energy charge exchange neutrals emitted from the center of the plasma would be attenuated as they travel through the rest of plasma. Because of these two effects, the experimental data would slightly deviate from the straight line given by Equation-9. To overcome this problem, only that portion of the curve for which E >> $3T_i$ (0) is used since attenuation is less for higher energy neutrals and contribution to energetic neutrals is less from the outer region of the plasma [5].

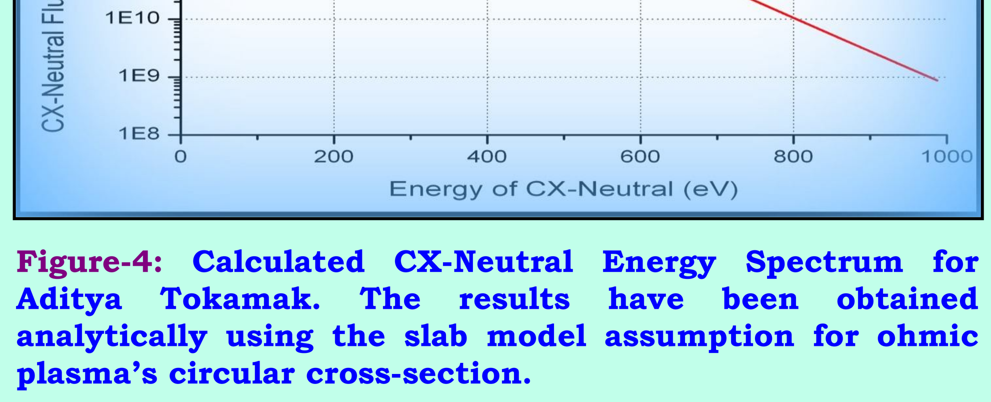

Figure-4: Calculated CX-Neutral Energy Spectrum for Aditya Tokamak. The results have been obtained analytically using the slab model assumption for ohmic plasma's circular cross-section.

Results and Discussion

The estimation of ion temperature with ADITYA plasma discharge number 22738 has been illustrated (Figures: 6, 7 and 8). Least square fitting of the straight line obtained by the plot of lnF Vs Energy was done and then the temperature was estimated as an averaged over 10 msec for each five such time intervals during flat-tops of Plasma Current I_p (Figure-5).

Figure-7 shows the temporal evolution of Electron temperature during ohmic heating and its comparison with Ion temperature data obtained using CX-NPA. It has been found that the peak ion temperature is typically 40% to 45% of the central electron temperature.

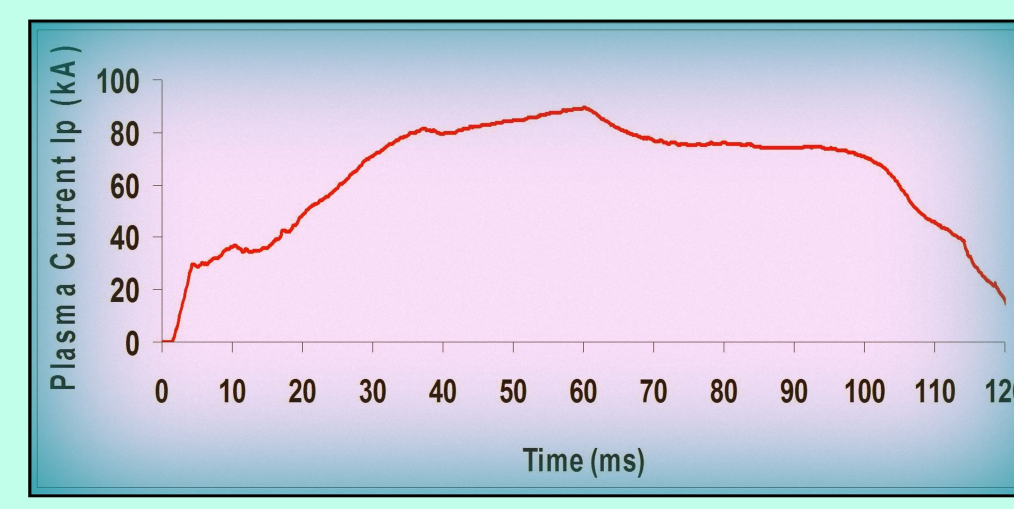

Figure-5: Plot shows evolution of plasma current with time during a typical plasma discharge in ADITYA.

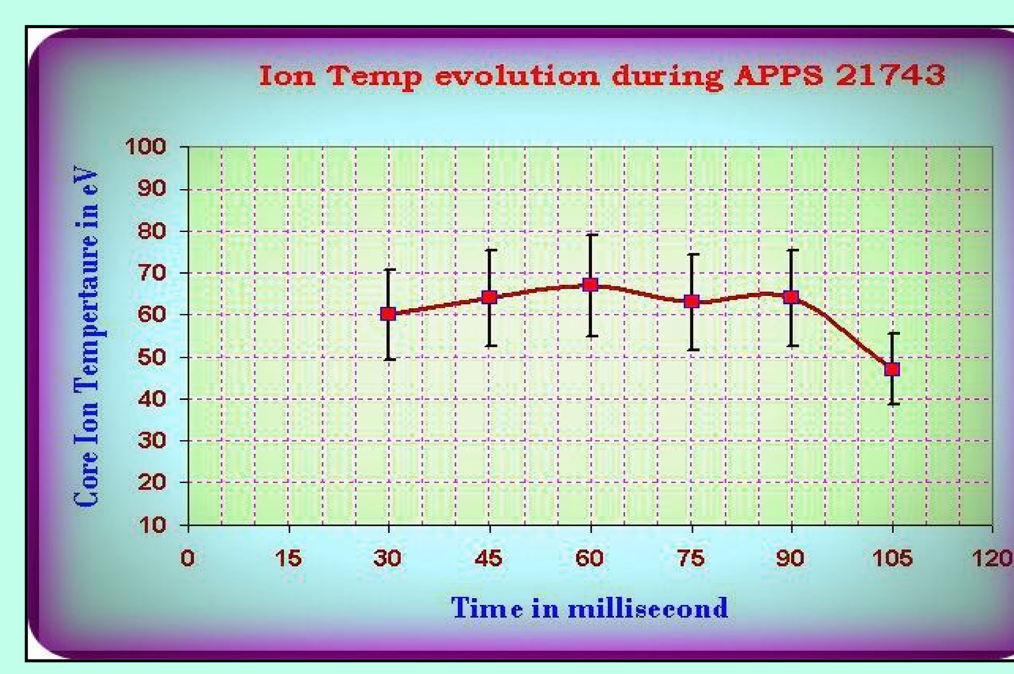

Figure-6: Plot shows temporal variation of central ion temperature T_i (0) during flat top of the current profile.

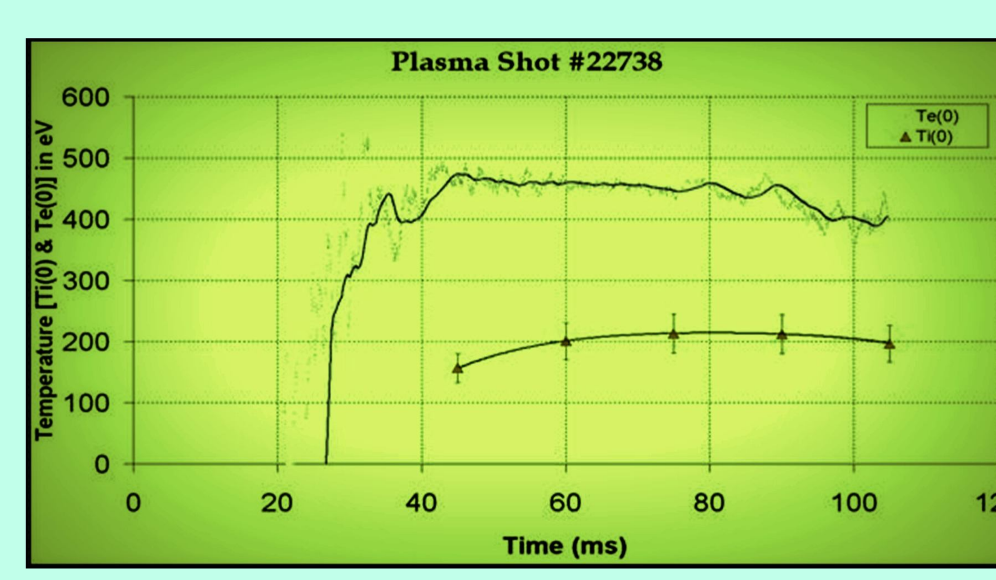

Figure-7: Plot shows temporal variation of central electron temperature Te(0) and central Ion temperature T_i (0).

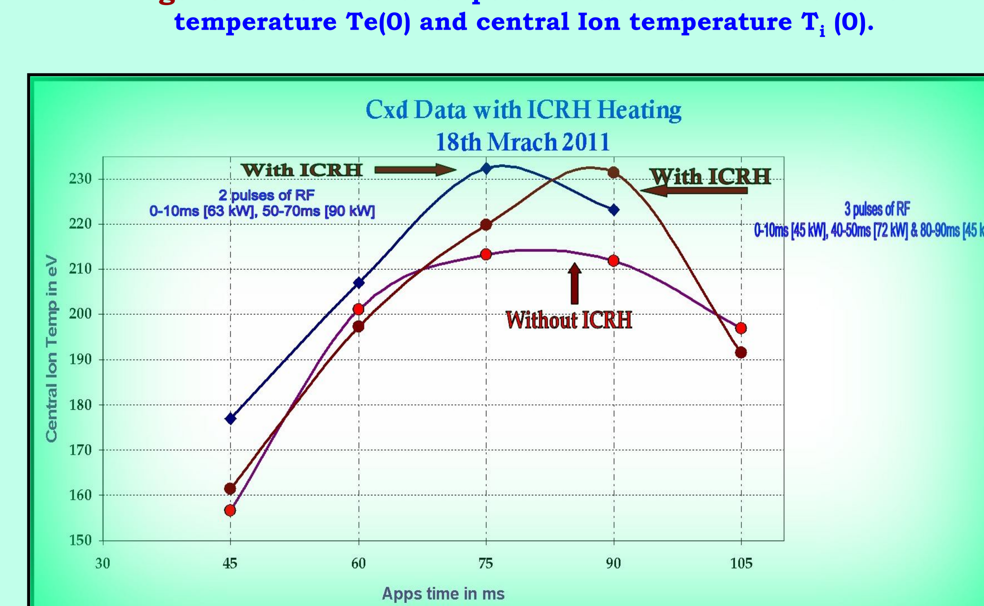

Figure-8: Plot shows temporal variation of central Ion temperature T_i (0) with applied RF heating.

Conclusion:

Passive CX-NPA is designed and developed for the Aditya tokamak ion temperature measurement. Energy calibrations of CX-NPA were carried out using low energy ion source and the results have been found to be in a good agreement with the calculated values.

Temporal evaluation of Ion temperature has been presented during the flat top of the plasma current and peak ion temperature for some recent APPS discharges were found to be typically 200 ± 40 eV. It has also been found that the peak ion temperature is typically 40% to 45% of the central electron temperature. The core ion temperature shows rise during the ICRH power , but the time resolution of data acquisition[at present 15 ms window] needs to be further improved for more detailed study of ion temperature variation.

References:

1. P.E. Stott, Nuclear Fusion, Vol. 32, No.1 (1992) p167.
2. V. V. Afrosimov, I. P. Gladkovskii, Yu. S. Gordeev, I. F. Kalinkevich, M. P. Petrov and N. V. Fedorenko: Soviet Phys.-Tech. Phys. 5 (1961) p1378.
3. Charles B. Wharton, A review of Energetic Neutral Particle Plasma Diagnostics, Laboratory of Plasma Studies, Cornell University, Ithaca (70).
4. G. A. Harrower, et. al., Rev. Sci. Instrum. Vol. 26, (1955), p850.
5. D D R Summers, et. al., J. Phys. E: Sci. Instrum., Vol. 11, (1978), p1183.
6. Amptektron Operating Maunal for CEM Model MD-50, Revision A2, August, 2005.
7. S. S. Medley, et. al., Rev. Sci. Instrum. Vol.79, 011101 (2008).
8. C. F. Barnett and J. A. Ray, A, Nucl. Fusion vol.12 (1972), p65.
9. C. J. Armentrout, et. al., Rev.Sci.Instrum. vol. 56, No.11 (1985), p2101.
10. R. Bartiromo et. al., Rev.Sci.Instrum. Vol. 58, No.5 (1987), p788.
11. S. L. Davis, et. al., Rev. Sci. Instrum. Vol. 54, No.03 (1983), p315.
12. Hiroshi Takeuchi, et.al, Jap. Journal of Applied Phy., Vol. 22, No.11 (1983), pp1709-1716.
13. Hiroshi Takeuchi, et. al, Jap. Journal of Applied Phy., Vol. 16 No.1, (1977), pp139-147.
14. T. Goto, et. al., Rev. Sci. Instrum., Vol. 70, No. 6 (1999), p2661.
15. G. Bracco, et. al., Rev. Sci. Instrum., Vol.63, No.12 (1992), p5685.
16. S. S. Medly, et. al., Rev. Sci. Instrum., Vol. 69, No.07 (1998), p2651.
17. Y. Nakashima, et. al., Rev. Sci. Instrum., Vol. 70, No.1, (1999), p849.
18. D. Brisson, et. al., Rev. ScI. Instrum., Vol.51, No.04, (1980), p511.
19. Hans H. Fleischmann et. al., Physical Review, Vol. 178, No. 1, (1969), p254.
20. N R Ray, J. Phys. D: Appl. Phys. 31 (1998), pp1071–1077.
21. D.E. Voss, et. al., Rev. Sci. Instrum., Vol. 53, No.11 (1982), p1696.
22. H. H. Fleischmann, Physical Review A, Vol. 10, No.2 (1974), 569.
23. T. A. Santosh Kumar, et. al., Technical Report: Aditya Charge Exchange Diagnostics, IPR/TR-56/96, February 1996